*J. Fluid Mech.* (2003), *vol.* 480, *pp.* 267–281.  
DOI: 10.1017/S0022112002003683 Printed in the United Kingdom

# Viscous fingering with chemical reaction: effect of *in-situ* production of surfactants

By JUAN FERNANDEZ AND G. M. HOMSY

Department of Mechanical and Environmental Engineering, University of California, Santa Barbara, CA 93106, USA

(Received 15 March 2002 and in revised form 25 September 2002)

Viscous fingering experiments are performed in a radial Hele-Shaw cell for a liquid–liquid system in the presence of a well-characterized interfacial reaction capable of changing the surface tension on the time scale of the experiments. The reaction is a neutralization of a fatty acid by an alkaline material to form a surfactant, which exhibits first-order kinetics for the surface tension as a function of time. The experiments are carried out for capillary numbers, $Ca$, high enough for the fingering to always be in the fractal regime, and for a wide range of Damköhler numbers, $Da$. The fingers are typically wider in the presence of the chemical reaction than the non-reactive case. We observe two different-behaviours of the reactive fingering patterns. For intermediate values of $Da$, $0.5 < Da < 4$, the fractal dimension $d_f$ is higher than the classical value measured for the non-reactive fingering patterns and reaches a maximum of about 1.9. For both small ($Da < 0.5$) and high $Da$ ($Da > 4$), the reactive fingering patterns are similar to the fingers with no reaction: the fractal dimension is found to be the same for both systems. These effects are consistent with the hypothesis that Marangoni stresses are present and produce wider fingers.

## 1. Introduction

An important emerging research area concerns the interaction between hydrodynamics and chemistry, in particular the influence of chemical reaction on hydrodynamic instabilities, such as the fingering instability originating from a difference in viscosity/density between two fluids. Most of these studies have focused on the buoyancy-driven instability from experimental (Carey, Morris & Kolodner 1996; Bockmann & Muller 2000) and theoretical (de Wit 2001) points of view. In this case, the chemical reaction produces a density gradient that can cause the front to be buoyantly unstable, giving rise to complex fingering phenomena. Of particular interest in the present work are the viscous fingering phenomena in immiscible systems in the presence of a chemical reaction at the interface. This situation is commonly encountered in various applications including secondary oil recovery, Hornof & Baig (1995), chromatographic separation, Matthew *et al.* (1997), and frontal polymerization, Pojman *et al.* (1998).

Since the seminal work of Saffman & Taylor (1958) and Hill (1952), viscous fingering has been the subject of numerous studies. The different mechanisms of splitting, shielding and spreading that govern the nonlinear propagation of fingers are discussed by Homsy (1987). In the case of immiscible displacements in Hele-Shaw cells, the viscous fingering instability is governed by the capillary number,

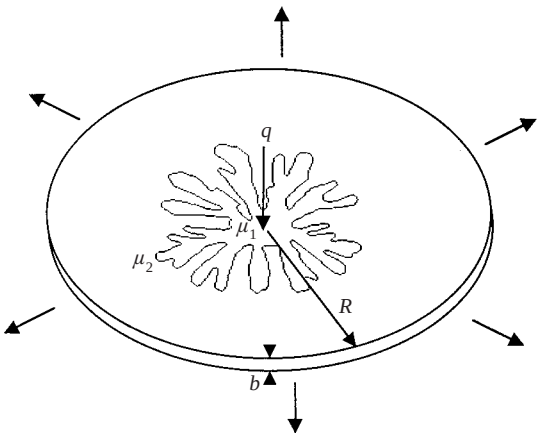


FIGURE 1. A schematic description of the radial flow in a Hele-Shaw cell. The flow is characterized by the capillary number $Ca$ and the mobility ratio $M = \mu_2/\mu_1$, with $\mu_1$ the viscosity of the less viscous fluid and $\mu_2$ the viscosity of the more viscous one.

$$Ca = \frac{\mu V}{\gamma}, \tag{1.1}$$

where $\mu$, $V$ and $\gamma$ are a characteristic viscosity, velocity and surface tension respectively. Of particular interest is the splitting of fingers which takes place over a range of length scales above a certain critical capillary number. Consider a radial Hele-Shaw cell as shown in figure 1. A less viscous fluid of viscosity $\mu_1$ is injected at the centre of the cell with a constant volume flow rate $q$. It displaces a second fluid of viscosity $\mu_2$. The resulting pattern depends on the capillary number and the mobility ratio $M = \mu_2/\mu_1$. Chen (1989) and Rauseo, Barnes & Maher (1987) have performed experiments in order to study the tip-splitting phenomena in a radial cell, at different capillary numbers defined for this geometry as

$$Ca' = \frac{\mu q}{\gamma b^2}. \tag{1.2}$$

Chen (1989) observed that the finger width scales with the capillary number as a power law, $Ca^{-m}$, where the exponent $m$ is found to be 0.31. This scaling has also been observed in a linear geometry by Kopf-Sill & Homsy (1987) with a slightly different exponent $m = 0.35$. These experimental measurements of $m$ are different from the prediction of linear stability analysis (Saffman & Taylor 1958; Chuoke, Meurs & Poel 1959), where the finger width is expected to scale as $Ca^{-1/2}$. This difference is explained by the stabilizing effect of the curvature of the finger (Kopf-Sill & Homsy 1987; Chen 1989). Chen (1989) measured the fractal dimension of the fingers. Above a critical capillary number, repeated tip-spitting leads to a fractal pattern at large times. May & Maher (1989) measured the fractal dimension of the fingering patterns for a wide range of capillary numbers. They found that the fractal dimension was approximately 1.71 for $Ca'$ between a critical value and 35. For intermediate values of $Ca'$ between 35 and 50 the fractal dimension increases to a value of 1.79, after which it does not change with further increase in capillary number.

These semi-classical results are significantly modified in the case of fingering in complex fluids. Recent experiments with non-Newtonian fluids in the presence of

surfactants show interesting changes in the viscous fingering patterns, see Bonn *et al.* (1995), Sastry *et al.* (2001). Both sets of experiments used a surfactant solution (water + SDS) where the surfactant concentration is above the critical micellar concentration (c.m.c.), and paraffin oil is the more viscous fluid. Both studies show that in rectilinear Hele-Shaw flows the finger width relative to the width of the channel is larger than the asymptotic limit of $\frac{1}{2}$ observed for the Saffman–Taylor finger at high capillary numbers. In a radial Hele-Shaw cell, Sastry *et al.* (2001) also observed that the fingers were wider than the standard patterns, with a fractal dimension of about 1.8.

Fingering patterns also change in the presence of chemical reactions. Our work is motivated by that of Nasr-El-Din *et al.* (1990), Hornof & Bernard (1992) and Hornof & Baig (1995), who performed viscous fingering experiments in the presence of a chemical reaction at the interface between a paraffin oil and water. Nasr-El-Din *et al.* (1990) and Hornof, Neale & Gholam-Hosseini (2000) have reported a series of reactive experiments in Hele-Shaw cells packed with glass beads. The reaction is seen to lower the interfacial tension by factors as high as 10–20 over a range of time scales from tens to thousands of seconds. The observed phenomena are complex due to the presence of the beads, the wide range of capillary number, the varying duration of the experiments, and the additional effects of wettability. Accordingly, no direct comparisons between their experiments and ours are possible. Hornof & Bernard (1992) conducted experiments in a so-called five-spot geometry at relatively low capillary numbers, $0.8 \leqslant Ca' \leqslant 7$, in which the alkaline solution was injected at one corner of the cell and the oil recovery was measured at the diagonal corner. They observed the formation of one finger for the reactive system which was wider than that in the non-reactive system of water/oil only. Hornof & Baig (1995) conducted similar experiments at fixed $Ca' = 0.38$ with varying mobility ratios. Oil recovery at breakthrough was higher (about 90% one hour after breakthrough) than in the non-reactive system. In addition, the long-time behaviour showed an increase in area swept by the aqueous phase (with a corresponding increase in recovery) relative to the non-reactive case. Hornof & Baig (1995) supposed that at the tip of the finger a new interface is generated having a lower surfactant concentration whereas, at the rear of the tip, the reaction has time to proceed so that the surface tension is no longer constant along the interface of the finger. As a consequence of this surface tension gradient, the instability is enhanced. We return to this point in § 4, but it is useful to note that these experiments were conducted at low flow rates well below the threshold for onset of fractal fingering. As such they were in a different regime than our experiments.

Despite this previous work, there has not been a study which systematically and quantitatively treats the issue of the relationship between fingering patterns and interfacial chemical kinetics. In this paper we present experiments on viscous fingering in the presence of a well-characterized interfacial chemical reaction whose kinetics we measure. We perform the experiments in a radial Hele-Shaw cell in the tip-splitting regime with the objective of studying the interaction between the viscous fingering patterns and the chemical reaction.

## 2. Experimental apparatus

Our experiments were conducted in a radial Hele-Shaw cell as sketched in figure 1. The cell consists of two circular plates of Plexiglas of 1.9 cm thick and 60 cm of diameter. The plates are separated by 12 plastic shim segments (4 cm × 12 cm) of 0.0318 cm in thickness placed uniformly along the circumference of the cell. Each

gasket is clamped between the plates by a cant-twist clamp in order to maintain a uniform gap thickness. The top plate has a small centre hole (1 cm diameter) drilled and tapped for injecting the fluids. The cell sits horizontally on a tray in which the fluids are collected for disposal. This arrangement allows the cell to be easily dismantled and reassembled in a way that ensures repeatability. A three-way valve is located at the inlet of the cell in order to avoid any mixing of the fluids before they enter the cell. The valve barrel switches from the filling position, when the cell is filled with the oil phase, to the dispense position, when the aqueous phase is injected at a given flow rate. The fluids are injected with a Masterflex peristaltic pump. In order to damp any pulsations caused by the pump, we connect a sealed glass flask which is half full of the injected solution between the pump and the cell.

The displaced fluid is paraffin oil and the injected fluid is millepore water. The reactants used in each fluid are described in § 2.1. The viscosity of the oil, measured using a Cannon-Fenske viscometer, is 1.6 P at room temperature (22°C). The aqueous solution is coloured by adding a small amount of potassium permanganate (about 0.2% of the total weight of the solution). The experimental procedure is as follows. After the cell is initially filled by the oil phase, the aqueous solution is injected at a constant and well-controlled flow rate by means of the variable speed peristaltic pump (Masterflex-Cole Parmer). The volume flow rate $q$ is varied from $0.14\,\mathrm{ml\,s^{-1}}$ to $1.45\,\mathrm{ml\,s^{-1}}$. The experiments are videotaped by a CCD camera with a 35 mm objective mounted vertically above the cell. The images are acquired at 5 frames $\mathrm{s^{-1}}$ using the ImageJ software with a resolution of 0.06 cm/pixel. This image analysis program is also used to measure the finger width and the fractal dimension of the patterns, as explained below.

We measure the gap thickness of the cell for the two extreme flow rates, $q = 0.14\,\mathrm{ml\,s^{-1}}$ and $q = 1.45\,\mathrm{ml\,s^{-1}}$, using the method proposed by Chen (1989). We measure the area of the interface between the oil and the air, which remains circular when the oil is the displacing fluid, as a function of time. For the low flow rates, the calculated gap width is found to be within 2% of the nominal value whereas at the highest flow rate, the measured gap is about 10% higher, probably due to the deflection of the Plexiglas plates. As we will see in § 3.1, the influence of this deflection can be neglected.

### 2.1. *Reactive system*

The neutralization of fatty acids by an alkaline material produces the corresponding carboxylic acid salts, which are anionic surfactants. This reaction is well known and widely used in various industries such as in soap fabrication and food processing, Rosen (1989). In our experiments, we add linoleic acid (fatty acid) to the paraffin oil and sodium hydroxide (NaOH) to the water. Accordingly when we inject the alkaline solution into the cell, the linoleic acid reacts with the sodium hydroxide at the water/oil interface, producing the corresponding surfactant *in-situ*.

In order to characterize the rate of production of surfactant, we have measured the time-dependent surface tension by the pendant drop method (Touhami, Hornof & Neale 1998) for the concentrations of reactants listed in table 1. The other quantities in table 1 will be defined shortly. The shape of a pendant drop is determined by a combination of the surface tension and gravity effects in which surface forces tend to make the drop spherical and gravity tends to elongate it. This balance is determined by the Bond number, $Bo = \Delta\rho g R^2/\gamma$, where $\Delta\rho$ is the density difference, $\gamma$ the surface tension and $R$ is the curvature of the drop at the apex. Figure 2 shows the shape evolution with time of a pendant drop of water/NaOH into a solution of oil/acid for

| | $C_{NaOH}$ (mol m$^{-3}$) | $C_{acid}$ (mol m$^{-3}$) | $\gamma_0$ (dyn cm$^{-1}$) | $\gamma_\infty$ (dyn cm$^{-1}$) | $k$ (s$^{-1}$) |
|---|---|---|---|---|---|
| System A | 125 | 0.1 | 48 | 10 | 0.05 |
| System B | 12.5 | 1 | 35 | 7 | 0.1 |

TABLE 1. Concentrations of the linoleic acid and the sodium hydroxide (NaOH) used in the experiments. The surface tension is measured by the pendant drop method. The various quantities are described in the text.

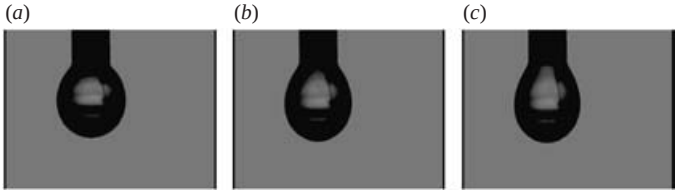


FIGURE 2. Images of a pendant drop of water/sodium hydroxide into paraffin oil/linoleic acid (system A) at different times. As the reaction proceeds, the surface tension decreases and results in an elongation of the drop shape. (*a*) $t = 10$ s, (*b*) $t = 60$ s, (*c*) $t = 100$ s.

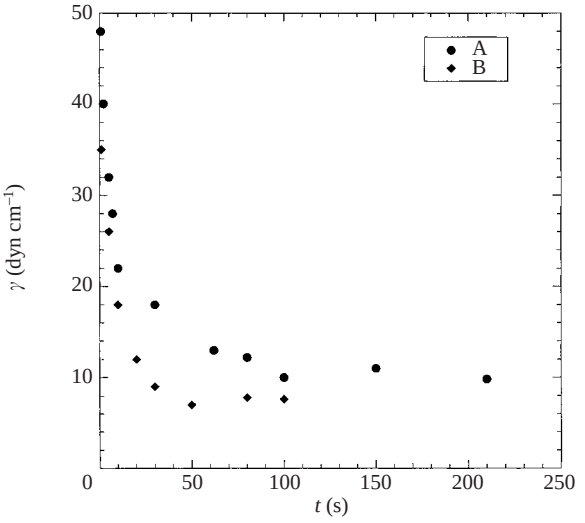


FIGURE 3. Typical evolution of the surface tension versus time. As the reaction proceeds, the surface tension decreases from $\gamma_0$ to a final steady value of $\gamma_\infty$.

the system A. We calculate the surface tension using the tables of Andreas, Hauser & Tucker (1938) which link the Bond number to the drop shape. The results are shown in figure 3, in which $t = 0$ is taken to be the time when the drop has been completely formed. As can be seen, the surface tension decreases with time as the reaction proceeds. At completion the surface tension reaches a constant value $\gamma_\infty$, which is lower than the initial surface tension $\gamma_0$. These quantities are reported in table 1 and are in good agreement with those of Touhami *et al.* (1998).

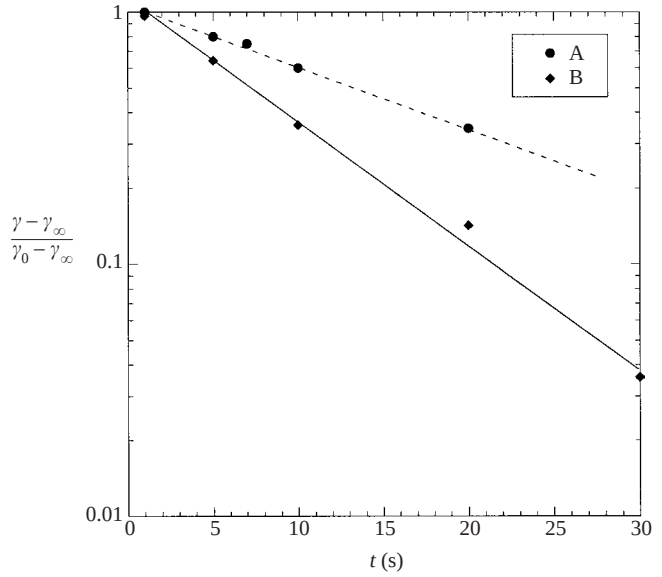


FIGURE 4. $(\gamma(t)-\gamma_\infty)/(\gamma_0-\gamma_\infty)$ versus time in a semi-logarithmic plot. The kinetic rate constant $k$ is determined by fitting an exponential law.

It is important to characterize the kinetics of the reaction over the duration of a given experiment. Accordingly, we normalize the decrease of the surface tension by the difference between the initial value $\gamma_0$ and the final value $\gamma_\infty$. As shown in figure 4, the decrease of the reduced surface tension exhibits a simple exponential decay. The resulting first-order kinetic rate constant $k$ is given in table 1 for the two concentrations used.

### 2.2. *Dimensional parameters*

We are interested in studying the interaction of the reaction with the fingering process. In order to do so, we need to establish the relevant length and time scales. We define the characteristic time as the nominal residence time:

$$t_R = \frac{b\,R^2}{2\,q}. \tag{2.1}$$

Here $R$ is the radius of the cell, $b$ is the gap thickness, and $q$ the volume flow rate. As mentioned in the introduction, the fingering phenomenon is characterized by the capillary number $Ca = \mu V/\gamma$, where $V$ is the instantaneous interface speed as defined below, $\mu$ is the viscosity of the more viscous fluid, and $\gamma$ is the surface tension. We will use the initial surface tension $\gamma_0$ in the definition of the capillary numbers (1.1) and (1.2) in order to compare the reactive flow with the standard flow where there is no reaction present. This choice is justified in the next section.

It is necessary to compare the chemical reaction rate against flow rates as follows. The Damköhler number $Da$ is defined as the ratio of the residence time to the characteristic time of the reaction $k^{-1}$,

$$Da \equiv k\,t_R = \frac{kbR^2}{2q}. \tag{2.2}$$

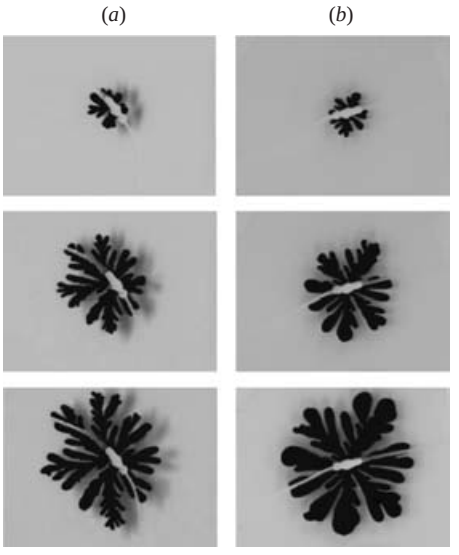


FIGURE 5. Images showing the evolution of viscous fingering patterns at $Ca' = 38$: (*a*) $Da = 0$, (*b*) Da = 0.6. Time is increasing from top to bottom: $t = 2, 10$ and 20 s.

The effect of chemical reaction on fingering is thus controlled by this parameter. At high values of *Da*, the reaction reaches completion very quickly and we expect classical fingering appropriate to the capillary number based on $\gamma_\infty$. On the other hand, at low Damköhler numbers, the reaction is very slow compared to the evolution of the fingering patterns so that we again expect classical fingering appropriate to a capillary number based on $\gamma_0$. At intermediate Damköhler numbers, the reaction is important over the duration of an experiment. Thus our experiments are characterized by the two dynamic parameters, *Ca* and *Da*, and the mobility ratio, *M*, which is held fixed at $M = 160$. In the case of standard viscous fingering ($Da = 0$), the experiments of Chen (1989) and Rauseo *et al.* (1987) showed that the fingering patterns undergo tip-splitting for high capillary numbers $Ca' \gg Ca'_{crit}$, where $Ca'_{crit} = 5$. In this regime, the fingers become fractal with essentially constant fractal dimension. All our experiments are performed at flow rates such that the fingering was always in the fractal regime.

## 3. Results

### 3.1. *Qualitative results*

Figure 5 shows three successive images of viscous fingering patterns for the standard and for the reactive systems for the same modified capillary number, $Ca' = 38$. For the non-reactive system, the fingers undergo a tip-splitting instability as expected at such high capillary numbers. For the reactive system, we observe no difference compared to the standard system at early times. The interface between the alkaline solution and the acidified oil splits to form fingers which give rise to different generations of tip-splitting. However, we note that the finger width increases as the chemical reaction proceeds, so that at completion of the experiment, the fingers are wider than those obtained in the non-reactive system. We also note that the reactive fingers are no longer subject to tip-splitting instability at late times, also leading to wider fingers. This inhibition of tip-splitting is systematically observed in the experiments where the reaction is present.

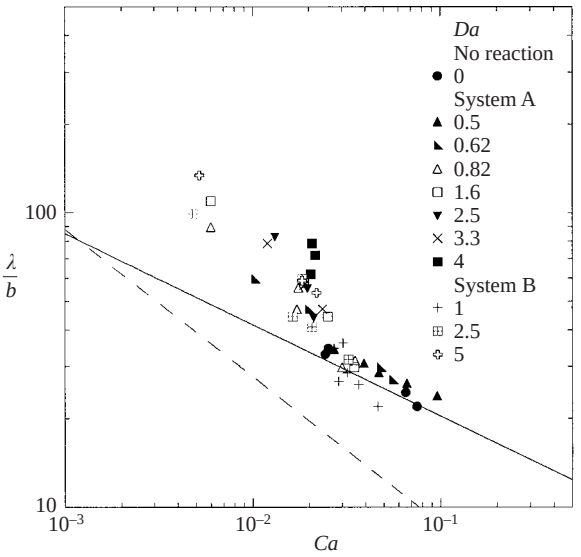


FIGURE 6. Experimental data $\lambda/b$ as a function of $Ca$ for the reactive and the non-reactive viscous fingering patterns: – – –, $2.78\,Ca^{-1/2}$; ——, $10\,Ca^{-0.31}$.

### 3.2. *Quantitative results: finger width*

We measured the splitting wavelength $\lambda$ or finger width defined as the width at the earliest indentation on a finger tip (Chen 1989). The finger speed $V$ at the moment $t$ of discernible indentation is taken to be the average of the speeds of the two new fingers,

$$V = \frac{r_t(t+\delta t) - r_t(t-\delta t)}{2\,\delta t}, \tag{3.1}$$

where $\delta t$ is the time interval between two consecutive images. We report the measurements as $\lambda/b$ as a function of the capillary number $Ca$ in figure 6. We perform experiments with no chemical reaction in order to compare our results with the classical results of Chen (1989) and Rauseo *et al.* (1987). Chen (1989) found that the normalized finger width $\lambda/b$ scales as $8.7\,Ca^{-0.31}$ for $5\times10^{-4} \ll Ca \ll 10^{-1}$. In this case, we find the same scaling of law as Chen (1989), as shown by the straight line in figure 6. The fit to our data is $\lambda/b = 10\,Ca^{-0.31}$: the proportionality constant is slightly higher than that measured by Chen (1989). This difference may be due to the slight deformation of the Plexiglas plates at the higher flow rates. The dashed line represents the scaling derived from the linear stability theory for a planar interface (Saffman & Taylor 1958; Chuoke *et al.* 1959). The fact that $\lambda/b$ does not scale as $Ca^{-1/2}$ shows the stabilizing effect of the finger curvature as discussed by Kopf-Sill & Homsy (1987) and Chen (1989).

Since $Ca$ is varied primarily by changing the flow rate, the data in figure 6 are also for varying $Da$. The departure from the scaling law is therefore due to chemical reaction. Since $Da$ is inversely proportional to flow rate (see 2.3), large $Ca$ corresponds to small $Da$ and vice versa. For the two reactive systems A and B listed in table 1, two different behaviours are observed. At low $Da$ ($Da < 0.5$) the normalized finger width $\lambda/b$ is similar to the finger width measured for the non-reactive system. When $Da$ increases ($Da > 0.5$), the finger width increases as seen by a departure of

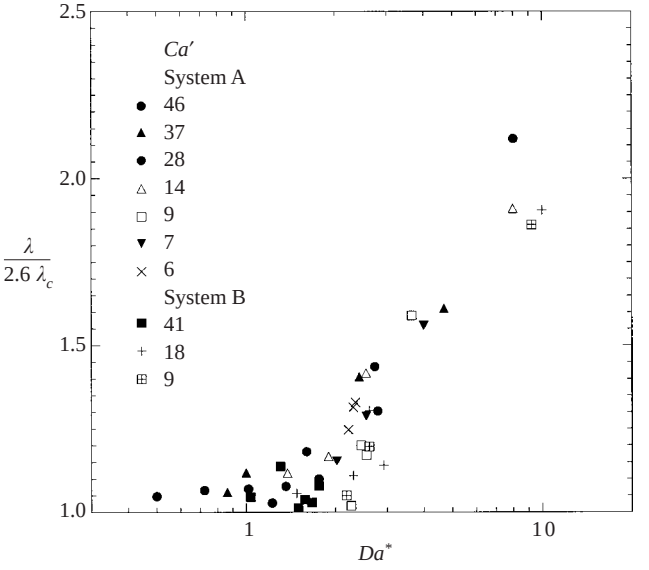


FIGURE 7. Measurements of $\lambda/2.6\,\lambda_c$ as a function of $Da^*$ for the reactive viscous fingering patterns.

$\lambda/b$ from the established scaling, characterized by a jump of $\lambda/b$ at $Ca = 0.025$. This value corresponds to a critical value of the Damköhler number as we show below.

Wilson (1975) and Paterson (1981) analysed the linear instability of an expanding circular interface when an inviscid fluid is displacing an immiscible viscous fluid at a constant volume flow rate $q$ in an Hele-Shaw cell. They showed that the fingers split as soon as their width becomes higher than a cut-off length $\lambda_c$ defined as

$$\lambda_c = \frac{2\pi r}{\left[(6/\pi)(r/b)Ca' + \frac{1}{4}\right]^{1/2} - \frac{1}{2}} \tag{3.2}$$

with $r$ the instantaneous radius of the interface. For the non-reactive system, we find that the finger width $\lambda$ is proportional to $\lambda_c$, $\lambda = 2.6\lambda_c$. This scaling is in good agreement with the experiments of Thome *et al.* (1989) with a sightly different value for the leading constant. Thus the increase in finger width in figure 6 must be due to chemical reaction.

By dimensional analysis, the finger width can be expressed as a function of the three dimensionless parameters:

$$\lambda = \lambda(Ca, Da, M).$$

We eliminate the dependence on $(Ca, M)$ by normalizing $\lambda$ by the new length scale, $2.6\,\lambda_c$, and plotting the results as a function of the instantaneous Damköhler number defined using the corresponding local velocity $V$ of the finger:

$$Da^* \equiv \frac{kR}{V} = \left(\frac{R\mu}{\gamma_0}\right) Ca^{-1}. \tag{3.3}$$

Figure 7 shows the results for the experiments performed with the two reactive systems A and B. We observe two characteristic regimes with a crossover at $Da^* = 2$. For low $Da^*$, the finger width is proportional to $\lambda_c$ as in the standard fingering case. As expected, the two reactive systems A and B are similar to the non-reactive system

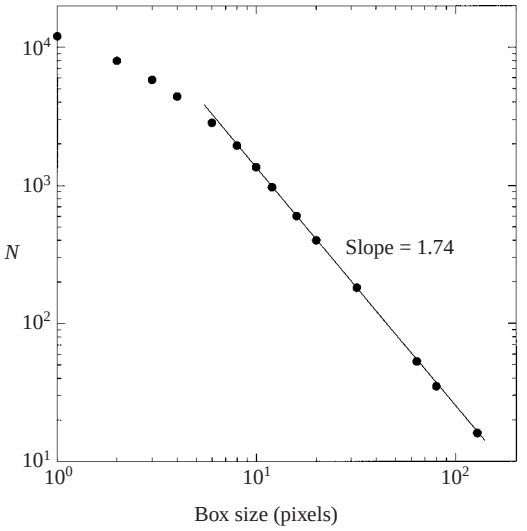


FIGURE 8. Fractal dimension $d_f$ of reactive fingering patterns (system A), in the tip-splitting regime ($Ca' = 47$) at low Damköhler number, $Da = 0.5$.

as there is no difference between the fingering patterns. More importantly, for high $Da^* \gg 2$ the finger width increases with $Da^*$. This crossover at $Da^* = 2$ leads to the jump of $\lambda/b$ at $Ca = 0.02$ that we observe in figure 6. In this regime of higher $Da^*$, the fingering patterns are governed by both $Ca$ and $Da$, with the primary observation that reaction generally results in wider fingers.

### 3.3. *Quantitative results: fractal dimension*

We measure the fractal dimension $d_f$ of the fingering patterns for all the experiments using the box counting method, Vicsek (1989). We count the number of square boxes $N$ necessary to cover the patterns as a function of the box size and we report the measurements in a log-log plot. An example is shown in figure 8 for reactive fingering patterns at low Damköhler number, $Da = 0.5$. In this case, we measure a fractal dimension of $1.74 \pm 0.02$. In this regime of low Damköhler numbers, the chemical reaction is very slow compared to the finger growth and the reactive fingers are similar to the non-reactive patterns as expected. Indeed, the value of $d_f$ that we measure compares well with the measurement of May & Maher (1989), $d_f = 1.75$, for the non-reactive fingering, at the same capillary number.

In the previous section, we observe that the fingering patterns become wider in the presence of the chemical reaction. This change is consistent with the temporal evolution for the fractal dimension of the reactive and the non-reactive cases, as shown in figure 9, for the same conditions as figure 5. For early times ($t < 5$ s), the fractal dimensions of both systems are similar. The reactive interface, like the non-reactive one, destabilizes into fingers which themselves split and give rise to second-generation splitting and so on. Therefore, $d_f$ decreases. At later times, as the reaction proceeds, the fractal dimension of the reactive system increases whereas for the non-reactive case, $d_f$ decreases towards the asymptotic value 1.74. The limiting value in the reactive case is 1.8. Indeed, as one can see in the bottom pictures of figure 5, the total area covered the reactive system is higher than in the standard system.

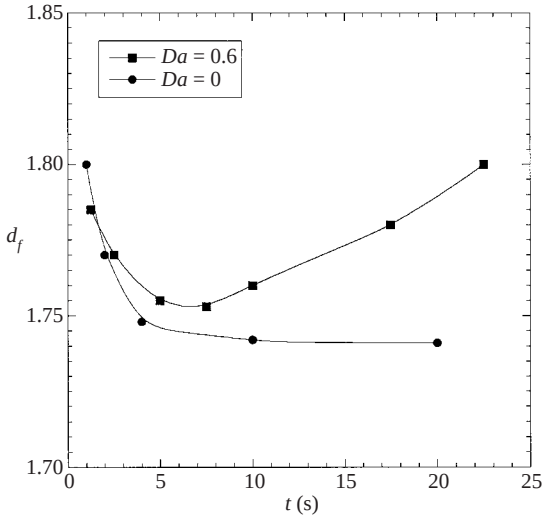


FIGURE 9. Temporal evolution of the fractal dimension of $d_f$ for the reactive system A ($Da = 0.6$) and for the standard fingering patterns ($Da = 0$) at $Ca' = 38$.

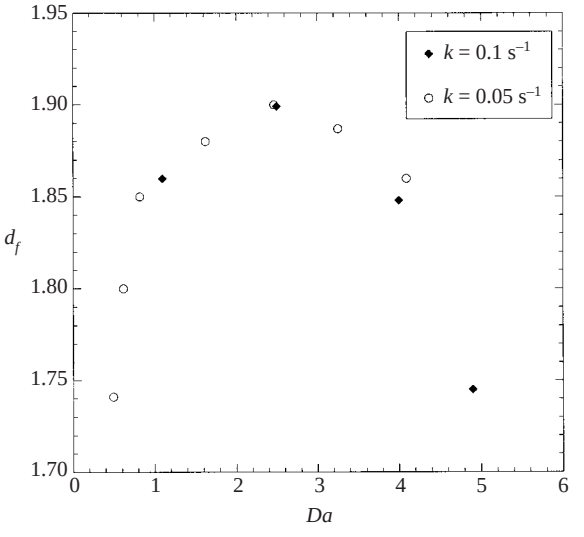


FIGURE 10. Fractal dimension $d_f$ as a function of $Da$.

In figure 10, we report the values of the fractal dimension for the two reactive systems A and B as a function of $Da$ (equation (2.2)). The measurements cover a wide range of Damköhler numbers, $0 \leqslant Da \leqslant 5$. As can be seen, $d_f$ scales as a unique function of $Da$. This is to be expected, since in the regime of our experiments, $d_f$ is independent of $Ca'$ (May & Maher 1989). As expected, we observe two different behaviours of the reactive fingering patterns. For low Damköhler numbers, $Da < 0.5$, the fractal dimension is the same as that with no reaction. Indeed, no changes in the fingering morphology are observed in the experiments. As $Da$ increases to intermediate values, $0.5 < Da < 4$, the fractal dimension $d_f$ is higher than for the non-reactive

fingering: $d_f$ increases and passes through a maximum of 1.9 at $Da = 2.4$. For $Da > 2.4$, $d_f$ decreases towards the standard value of non-reactive fingering. In this range of $Da$, the chemical reaction proceeds to completion earlier the higher $Da$. Indeed, at high values of the Damköhler number, $Da > 4$, the reaction has reached completion at very early times of the experiment. The fingering patterns are then similar to non-reactive patterns and we measure a fractal dimension very close to the standard value of 1.74.

## 4. Discussion and conclusion

We have performed experiments on viscous fingering in the presence of a chemical reaction taking place at the interface. The reaction produces surfactants *in-situ* that change the surface tension. The experiments, performed in the tip-splitting regime, cover a wide range of Damköhler numbers $Da$.

Our experiments show that the reactive fingering patterns are governed by the Damköhler number, unlike the standard viscous fingering which is characterized by solely the capillary number $Ca$. Additionally, all measurements have been shown to scale with $Da$. Although this is expected from dimensional analysis, ours are the first experiments to demonstrate it. In the presence of the reaction, the fingering patterns are wider than standard fingers. We observe that the finger width is determined by $Da^*$ for $Da^*$ above a critical value $Da^*_{crit} = 2$. For low Damköhler numbers, $Da^* < Da^*_{crit}$, the finger width scales with the capillary number, as for the standard fingering with no reaction. Moreover, the evolution of the fractal dimension as a function of the Damköhler number emphasizes two different behaviours of the reactive fingers. For $Da < 0.5$ and $Da > 4$, the fractal dimension of the reactive fingering patterns is similar to that of standard fingering, whereas for intermediate range $0.5 < Da < 4$, the fractal dimension is higher as the coverage of the reactive finger increases.

Hornof & Baig (1995) have speculated that these effects are due to Marangoni stresses acting on the finger. Our experiments, done under carefully characterized conditions with a reaction that produces a known surfactant, are consistent with that speculation, but in a slightly different way. In order for Marangoni stresses to be operative, there must be a gradient in surfactant concentration which may arise either due to interface dilation or to unequal rates of chemical reaction at different places on the interface. Hornof & Baig (1995) suppose that interface dilatation is important, leading to a higher interfacial tension at the finger tips. However, the Marangoni stress so created would cause flow *toward* the tip, which would not cause wider fingers. On the contrary, we hypothesize that, due to diffusional limitations in the troughs, the reaction goes to higher completion near the tips of the fingers than in the troughs, leading to a lower interfacial tension at the tips. The Marangoni stress so produced will cause flow from regions of low tension to high, i.e. from the tip to the trough. Such a flow will then act to spread the finger laterally, and represents an effect that is entirely absent without reaction. This hypothesis is consistent with our observation that the finger propagation is the same at short times for both reactive and unreactive cases – the pattern needs to develop some structure before diffusional limitations can limit the extent of reaction in the trough regions.

We have made estimates of the increased lateral spreading of the fingers as follows. At any given time, the rate of change of cross-sectional area of the pattern can be estimated by finite-differencing two images closely spaced in time. The results are shown in figure 11, where we plot the rate of change of area, $\mathrm{d}A/\mathrm{d}t$, vs. time for both the reactive and non-reactive cases. As can be seen, there is a small difference in the

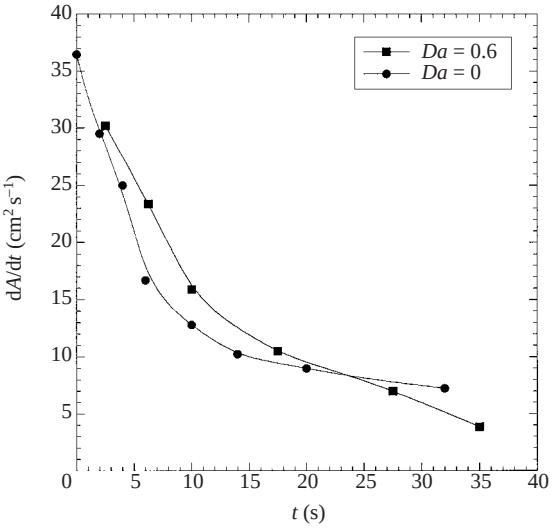


FIGURE 11. Rate of change of area $\mathrm{d}A/\mathrm{d}t$ versus time for the reactive ($Da = 0.6$) and the non-reactive case ($Da = 0$) at the same capillary number $Ca' = 38$. The curves are to guide the eye.

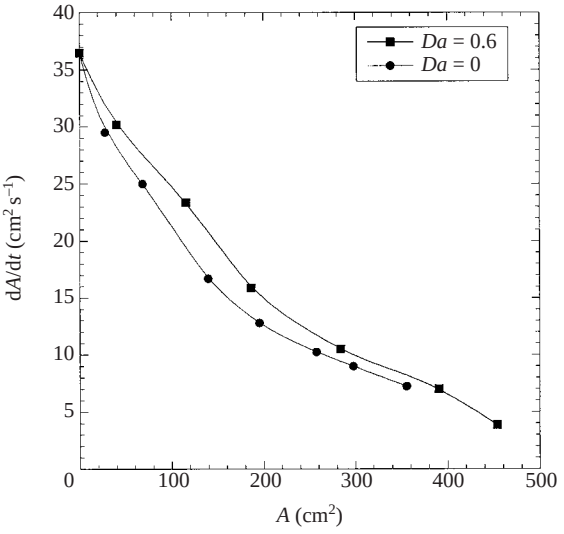


FIGURE 12. $\mathrm{d}A/\mathrm{d}t$ versus the instantaneous area $A$. The curves are to guide the eye.

rate of growth of area, the reactive case being the faster of the two. Since the patterns have evolved to different areas and configurations at any given time, we have also plotted $\mathrm{d}A/\mathrm{d}t$ vs. the instantaneous area, $A(t)$, in figure 12. The conclusion is that at a given area, the flow is producing area at a slightly faster rate for the reactive case, consistent with the higher fractal dimension.

We use the data in figure 12 to compute the difference in flux, $\Delta q$, in $\mathrm{cm}^3\,\mathrm{s}^{-1}$. These results are displayed as a function of area in figure 13, and show that the increased flux due to reaction varies with area covered, (time), but is between 0.02 and 0.06 $\mathrm{cm}^3\,\mathrm{s}^{-1}$. This is to be compared with the expected order of magnitude of the Marangoni flux, estimated as $\Delta\gamma b^2/\mu_2$. Assuming complete diffusional limitation in

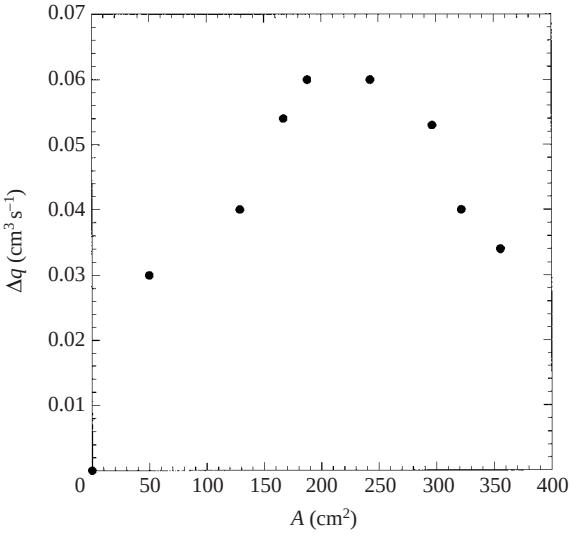


FIGURE 13. $\Delta q$ versus the instantaneous area $A$.

the trough of the finger, we estimate this quantity to be $0.02\,\mathrm{cm}^3\,\mathrm{s}^{-1}$, in reasonable agreement (in order of magnitude) with the measurements, giving quantitative support to the hypothesis. Further assessment of the hypothesis must await the development of a predictive mathematical model.

This work was supported by the Office of Basic Energy Sciences, US Department of Energy. We thank one of the referees for suggesting the calculations displayed in figures 11–13 .

## REFERENCES

ANDREAS, J. M., HAUSER, E. A. & TUCKER, W. B. 1938 Boundary tension by pendant drops. *J. Chem. Phys.* **42**, 1001–1019.

BÖCKMANN, M. & MÜLLER, S. C. 2000 Growth rates of the buoyancy-driven instability of an autocatalytic reaction front in a narrow cell. *Phys. Rev. Lett.* **85**, 2506–2509.

BONN, D., KELLAY, H., BEN AMAR, M. & MEUNIER, J. 1995 Viscous finger widening with surfactants and polymers. *Phys. Rev. Lett.* **75**, 2132–2135.

CAREY, M. R., MORRIS, S. W. & KOLODNER, P. 1996 Convective fingering of an autocatalytic reaction front. *Phys. Rev.* E **53**, 6012–6015.

CHEN, J.-D. 1989 Growth of radial viscous fingers in a Hele-Shaw cell. *J. Fluid Mech.* **201**, 223–242.

CHUOKE, R. L., VAN MEURS, P. & VAN DER POEL, C. 1959 The instability of slow, immiscible, viscous liquid–liquid displacements in permeable media. *Petrol. Trans. AIME* **216**, 188–194.

HILL, S. 1952 Channelling in packed columns. *Chem. Engng. Sci.* **1**, 247–253.

HOMSY, G. M. 1987 Viscous fingering in porous media. *Annu. Rev. Fluid Mech.* **19**, 271–331.

HORNOF, V. & BAIG, F. U. 1995 Influence of interfacial reaction and mobility ratio on the displacement of oil in a Hele-Shaw cell. *Exps. Fluids* **18**, 448–453.

HORNOF, V. & BERNARD, C. 1992 Effect of interfacial reaction on immiscible displacement in Hele-Shaw cells. *Exps. Fluids* **12**, 425–426.

HORNOF, V., NEALE, G. H. & GHOLAM-HOSSEINI, M. 2000 Effects of flow rate and alkali-to-acid ratio on the displacement of acidic oil by alkaline solutions in radial porous media. *J. Colloid Interface Sci.* **231**, 196–198.

KOPF-SILL, A. & HOMSY, G. M. 1987 Nonlinear unstable viscous fingers in Hele-Shaw flows. I. Experiments. *Phys. Fluids* **31**, 242–249.

Matthew, L., Dickson, T., Norton, T. T. & Fernandez, E. J. 1997 Chemical imaging of multicomponent viscous fingering in chromatography. *AIChE J.* **43**, 409–418.

May, S. E. & Maher, J. V. 1989 Fractal dimension of radial fingering patterns. *Phys. Rev.* A **40**, 1723–1726.

Nasr-El-Din, H., Khulbe, K. C., Hornof, V. & Neale, G. H. 1990 Effects of interfacial reaction on the radial displacement of oil by alkaline solutions. *Rev. Inst. Fr. Petrole* **45**, 231–243.

Paterson, L. 1981 Radial fingering in a Hele-Shaw cell. *J. Fluid Mech.* **113**, 513–529.

Pojman, J. A., Gunn, G., Patterson, C., Owens, J. & Simmons, C. 1998 Frontal dispersion polymerization. *J. Phys. Chem.* B **102**, 3927–3929.

Rauseo, S. N., Barnes, P. D. & Maher, J. V. 1987 Development of radial fingering patterns. *Phys. Rev.* A **35**, 1245–1251.

Rosen, J. M. 1989 *Surfactants and Interfacial Phenomena.* Wiley.

Saffman, P. G. & Taylor, G. I. 1958 The penetration of a fluid into a porous medium or Hele-Shaw cell containing a more viscous liquid. *Proc. R. Soc. Lond.* A **245**, 312–329.

Sastry, M., Gole, A., Banpurkar, A. G., Limaye, A. V. & Ogale, S. B. 2001 Variation in viscous fingering pattern morphology due to surfactant-mediated interfacial recognition events. *Current Sci.* **81**, 191–193.

Thome, H., Rabaud, M., Hakim, V. & Couder, Y. 1989 The Saffman–Taylor instability; from the linear to the circular geometry. *Phys. Fluids* A **1**, 224–240.

Touhami, Y., Hornof, V. & Neale, G. H. 1998 Dynamic interfacial tension behaviour of acidified oil/surfactant enhanced alkaline systems – 1. Experimental studies. *Coll. Surf.* A **132**, 61–74.

Vicsek, T. 1989 *Fractal Growth Phenomena.* World Scientific.

Wilson, S. D. R. 1975 A note on the measurement of dynamic contact angles. *J. Colloid Interface Sci.* **51**, 532–534.

de Wit, A. 2001 Fingering of chemical fronts in porous media. *Phys. Rev. Lett.* **87**, 054502.